Aerodynamic Analysis by CFD Simulation VS Wind-Tunnel Test to reduce Drag of UAV Aircraft

Mahmoud Abo El-Naga
Institute of Aviation Engineering and Technology, Giza, Egypt
mhmoud_shkawa@yahoo.com

Abstract– This work proposes an effective numerical models based on the Computational Fluid Dynamics (CFD) approach VS Wind-tunnel Measurements to obtain the optimum Drag reduction, by studying flow dynamics around a UAV plane with different shapes of (nose cones & boat tails). The experimental work of the test vehicle and grid system is constructed by ANSYS-16.2 FLUENT which is the CFD solver & employed in the present work. In this study, numerical iterations are completed, then after aerodynamic data and detailed complicated flow dynamics are visualized. In the present work, model of the UAV has been designed & developed in solid works-18 and generated the wind tunnel and applied the boundary conditions in ANSYS workbench 16.2 platform then after testing and simulation has been performed for the evaluation of drag coefficient for the UAV. In another case, the aerodynamics of the most suitable three designs of (nose cones & boat tails) is introduced to be manufactured for the Wind-tunnel Measurements evaluation in full scale Wind-Tunnel for the optimum drag coefficient for this UAV by comparison between both data of (CFD) and Wind-tunnel Measurements. Erasing the stagnation faces is totally reduces drag in head-on wind and bring about the significant improvements in the aerodynamic efficiency of the UAV planes with Streamlined shapes, it can be obtained. Hence, the drag force can be reduced by using add on parts on vehicles and fuel economy, battery economy and stability of a planes can be improved [1].

Keywords-- Drag Reduction, Wind-Tunnel Test, ANSYS FLUENT, CFD Simulation, Drag Coefficient.

I. INTRODUCTION

"Aerodynamics is the study of a solid body moving through the atmosphere and the interaction which takes place between the body surfaces and the surrounding air with varying relative wind direction" [6]

Therefore, if the interests of sizing, configuration & structure teams are to design a fuselage with light weight with strength structure and suitable volume, then the priority for the aerodynamics team is to care about the final shape of the moving air vehicle and its dynamic ability while flying so, in this article after defining the drag force and it's types, we will presenting the final shape of the fuselage structure with different shapes of (nose cones & boat tails) detailed drawn on slidworks-18 preparing to simulated computationally on ANSYS-16.2 software (by importing the geometry from solid works, meshing & setup) and compare the result with wind-tunnel experimental data trying to find the optimum shape in several flight speeds as detailed explained. The paper also presents wind-tunnel tests [9] and CFD numerical aerodynamic analysis of UAV aircraft. An extensive wind tunnel tests campaign of several different modular aircraft configurations analyzed has been performed on a full-scale model in order to experimentally estimate both longitudinal and lateral-directional stability, aerodynamic derivatives, and to improve the aircraft aerodynamic performances. Simultaneously numerical investigations through a CFD software have been performed, at wind-tunnel tests Reynolds number (Re=0.6millions) is a free flight Reynolds number of the full-scale aircraft. Finally, results are compared showing a good agreement in underestimation of drag coefficient in both CFD numerical analysis and wind-tunnel tests [4].

Total Drag

The total drag isn't simply the sum of the drag of each component, because when the components are combined into complete configuration can affect the flow field, and hence, the drag of another [1].

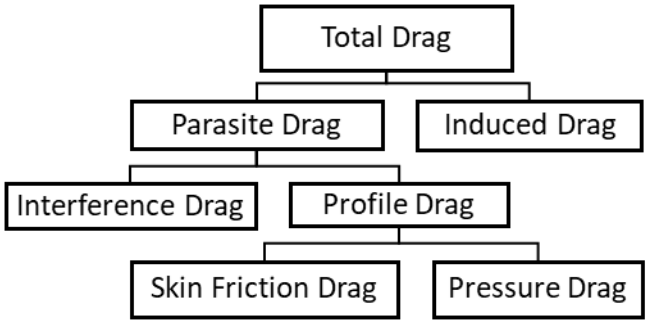

Figure 1 Drag decomposition.

Induced Drag

The induced drag is a pressure drag caused by the induced flow (downwash) associated with the vortices created at the tips of rocket fins.

Parasite Drag

The drag used for the profile drag for complete vehicle, integrated over the complete rocket surface.

Interference Drag

An additional pressure drag caused by mutual interaction of the flow fields around each component of the rocket. Can be minimized by proper fairing & filleting which induces smooth mixing of air past the component.

Profile Drag

It is the total drag on an aerodynamic shape due to viscous effect, it is sum of skin-friction & form drag that both come due to the shape & size of the rocket body so it is called profile drag.

Skin-friction Drag

It is the drag due to shear stress and flow viscosity integrated over the surface (Boundary layer effect).

Form Drag

This is the drag that is generated by the resolved components of the force due to pressure imbalance acting normal to the surface at all points, caused by flow separation.

Wave Drag

This is the drag associated with the formation of Oblique & Normal shock waves at high speeds, it represents the effect of compressibility in Transonic & Supersonic flow.

II. Problem Setup

We can show the final shape of our UAV to know that the **Form Drag** is our target to be reduced by reducing the stagnation faces and expansion areas.

A. Mathematical Model

The present problem is modeled as compressible, non-isothermal, turbulent, unsteady ideal gas flow with dispersed incompressible constant diameter cough-generated aerosols. The numerical simulation was done using ANSYS FLUENT 16.2 software on baseline square back UAV model of 1:1 scale. Averaged Navier- Stokes's equation was employed in this study and CFD simulation was preferred because of its low cost and time saving over wind tunnel experiments [2].

B. Geometry

The geometry of the UAV fuselage under consideration is demonstrated in Figure 2. The UAV basic fuselage contains two tapered parts, the front is 101 deg with the vertical line & the rear one is 80 deg with horizontal line. The frontal **stagnation** Area = 3600 mm^2 and the End **expansion** Area = 2500 mm^2 attached in a Tail Boom with Diameter = 25 mm.

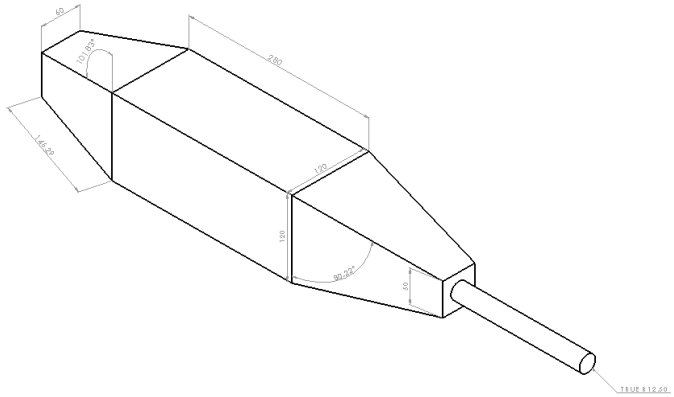

Figure 2 Geometry of the basic UAV configuration.

The solid CAD model of a UAV fuselage was created in SolidWorks-18. The solid model was then saved as a STEP file and then imported to Ansys Fluent 16.2 workbench for further analysis.

C. mesh

The meshing sizing is as follows: Mesh element is smooth and fine, the size for all the mouths and faces is 5 mm, 20 mm on the bodies, and 50 mm for the rest of the computational domain. Hence, the total number of elements is 7.8 million. The mesh is demonstrated in Figure 3.

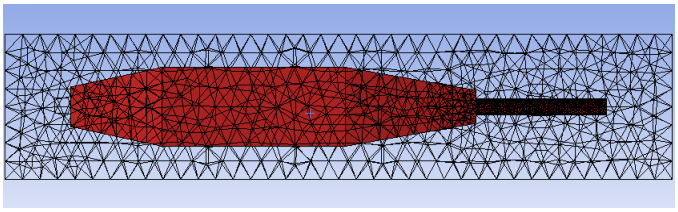

Figure 3 side view of the used mesh on basic fuselage.

D. Boundary Conditions

The following boundary conditions for the flow problem were used for the simulation can be summarized as follows:

Table 1 Boundary conditions

Boundary		Condition
Inlet	Velocity	5 m/s**:** 25 m/s
	Density	1.225 Kg/m^3
	Temperature	288 K
Body	Temperature	Adiabatic
	Velocity	No slip

The solution for the mathematical algorithm used was the Simple algorithm for the iterative solution of the steady RANS equations and the algorithm was of second order upwind scheme in spatial discretization [3].

E. Studied Cases

We draw all the modification parts under specific design concept taking the fuselage slopes in our consideration. We draw four different shapes of noses shown in Figure 4 with [H.nose, F.nose, R.nose & S.nose] as shown in Respectively.

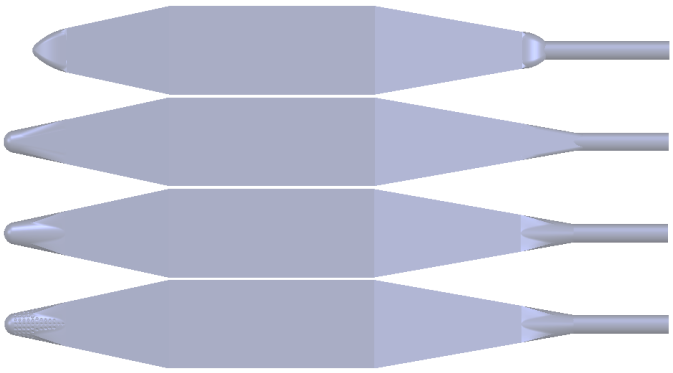

Figure 4 All configurations of the UAV modified parts.

III. Results and Discussions

A. CFD Simulation

After simulating the problem using ANSYS FLUENT, separately the results are summarized in Table 2 and Table 3.

Table 2 Drag Coefficient with Noses Only

Velocity	Base	H.nose	R.nose	F.nose
5	0.036024	0.02415	0.02314	0.02424
10	0.12947	0.08299	0.08182	0.08359
15	0.27713	0.17252	0.17164	0.17382
20	0.48136	0.26419	0.28849	0.29821
25	0.74072	0.62432	0.61653	0.62741

It is shown that the Drag decreases in all speeds with noses only as chart in Figure 5.

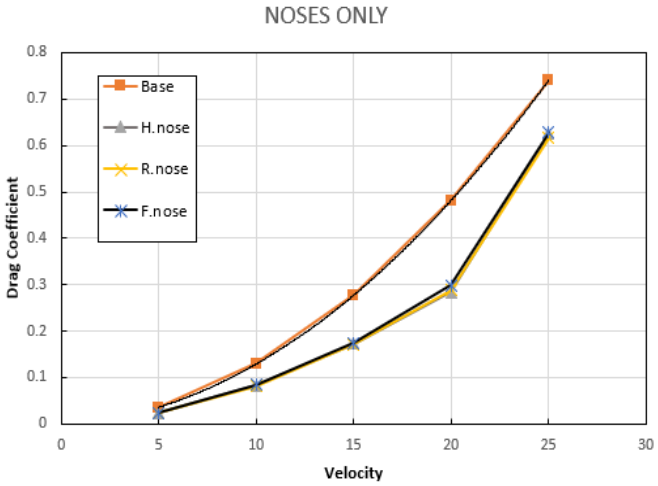

Figure 5 All configurations of the UAV modified noses only.

When we simulated the Full Body shapes with nose cones & boat tails its shows that values.

Table 3 Drag Coefficient with Full Body

Velocity	Base	H.body	R.body	F.body
5	0.036024	0.02304	0.02274	0.02409
10	0.12947	0.07877	0.07839	0.08333
15	0.27713	0.1633	0.16297	0.16452
20	0.48136	0.27898	0.27746	0.27991
25	0.74072	0.43215	0.42439	0.43376

We found that the optimum shape to use from the CFD simulations is **[R.Nose]** as shown in the chart viewed in Figure 6 for all cases, Hint: the (S.nose) can not be simulated because its hard meshing in the mesh solver process based on its complicated designed shape.

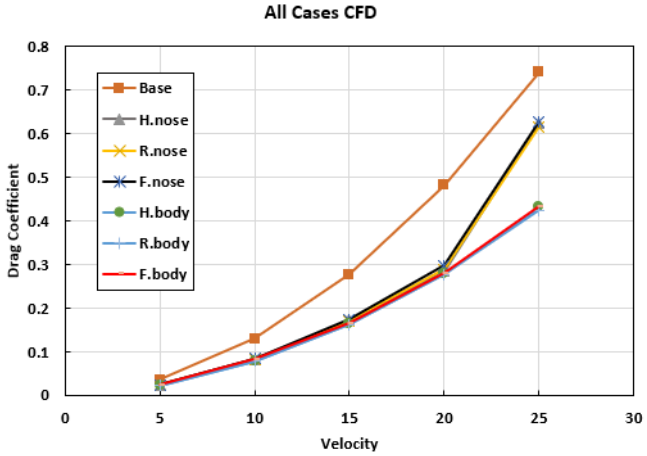

Figure 6 All configurations of the UAV simulated on CFD.

B. Wind-Tunnel Experiment

We started preparing to the wind-tunnel experiment by constructing the fuselage from 3 mm thickness wood which cut on CNC machine (laser cutting) contains four side skins (same size) & four main Frame's structure support assembled as shown in the wind-tunnel test section in Figure 7 [7].

Figure 7 Wind-Tunnel with the basic model in the test section.

For the modification parts construction we use 3D Printer to achieve high accuracy and excellent surface finish, because it uses SUNLU PLA Filament plastic or polylactic acid is a vegetable-based plastic material, which commonly uses cornstarch as a raw material as shown in Figure 8.

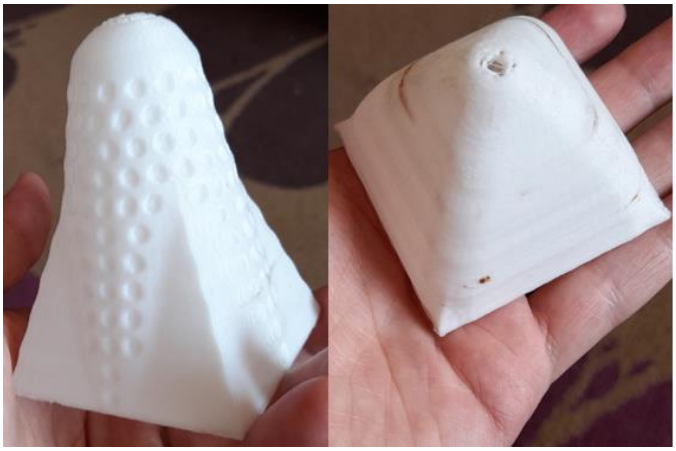

Figure 8 Sample of 3D Printed nose cones [S.nose & H.nose].

After testing the all cases separately under the same condition for each speed we summarize a very hard work in the shown chart Figure 9 to find the optimum shape is [R.Nose] from wind-tunnel experiment too.

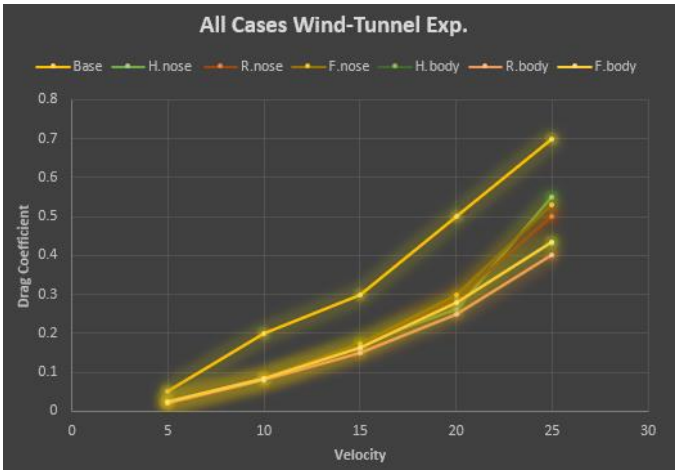

Figure 9 All configurations of the UAV tested on Wind-tunnel result.

IV. CONCLUSION

The results obtained through wind tunnel experiments and CFD simulations of the base model showed very good agreement with a small deviation at wind tunnel tests results V = 25 m/s. The addition of a (nose cones & boat tails) changed the flow structure and shifted the graph of static pressure distribution up and this improved the balance of pressure at the front part and rear part of the UAV with reference to the atmospheric pressure line. This resulted in the reduction of drag coefficient by 57.64% at 20 m/s. Due to this change in the static pressure variation on the flow structure there was a relatively small increment in the lift coefficient and was found to be less than 1.5%. The pressure distribution results from 16-tapping points [10] around the centreline profile of the UAV model [5] showed a separation at the rear and pressure failed to recover in that area for the base model. This failure to recover pressure resulted in the formation of aerodynamic drag. The addition of a (nose cones & boat tail) resulted in the control of the rear wake and a front shift in the static pressure distribution as depicted from the plots. The control of the flow field structure resulted in the reduction of drag and better (fuel economy or battery economy) [8]. However, the reduction of drag came with a reward of increasing lift which leads to increase plane stability at low speeds.

REFERENCES

[1] https://www.academia.edu/44739666/Advanced_High_Power_Rockets

[2] Çengel, Y., & Cimbala, J. M. (2005). *Fluid Mechanics:* Fundamentals and Applications. McGraw-Hill.

[3] Department of Aeronautical Engineering, Universidad Nacional Experimental Politécnica de la Fuerza Armada, Maracay, Venezuela, 2003.

[4] Cárdenas, E., Boschetti, P., Amerio, A., and Velásquez, C., "Design of an Unmanned Aerial Vehicle for Ecological Conservation," AIAA Paper 2005-7056, Sep. 2005.

[5] Boschetti, P. J., Cárdenas, E. M., and Amerio, A., "Drag Clean-Up Process of Unmanned Airplane for Ecological Conservation," Aerotecnica Missile e Spazio, Vol. 85, No. 2, 2006, pp. 53-62.

[6] Anderson, J. D., Aircraft Performance and Design, Mc Graw-Hill International Edition, Singapore, 1999, pp. 296-305.
[7] Giordano V., Coiro D.P., Nicolosi F. Reconnaissance Very Light Aircraft Design. Wind-Tunnel and Numerical Investigation, *Engineering Mechanics*, Vol. 7, No. 2, pp. 93-107, 2000. ISSN 1210-2717.
[8] Coiro D.P., Nicolosi F. Aircraft Design through Numerical and Experimental Techniques Developed at DPA, *Aircraft Design Journal*, Vol. 4, No. 1, March 2001, ISSN 1369-8869.
[9] Barlow J.B., RAE W.H., POPE A., Low-speed wind tunnel testing, 1984, John Wiley & Sons, Inc.
[10] Rumsey C L, Long M, Stuever R A and Wayman T R. Summary of the First AIAA CFD High Lift Prediction Workshop. AIAA-2011-839, American Institute of Aeronautics and Astronautics, 2011.